Research on methanol-tolerant catalysts for the oxygen reduction reaction
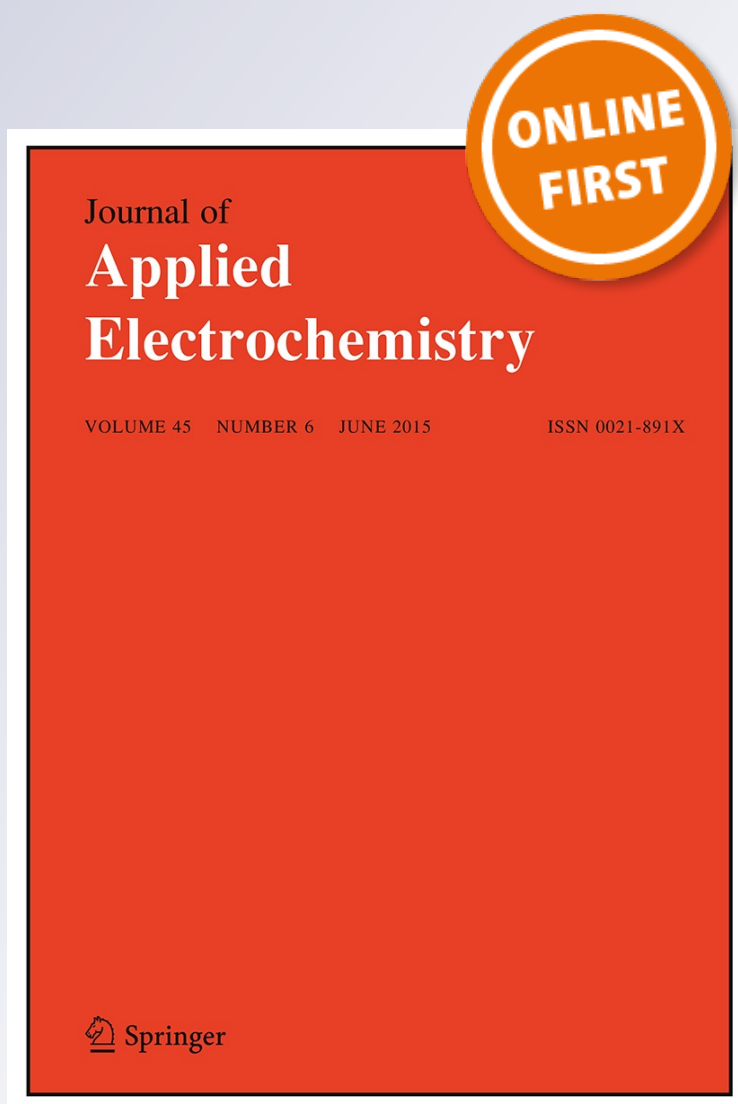
M. Asteazaran, G. Cespedes, S. Bengió, M. S. Moreno, W. E. Triaca & A. M. Castro Luna

Journal of
Applied
Electrochemistry

ONLINE FIRST

🗇 Springer

🗇 Springer

Springer

CrossMark

RESEARCH ARTICLE

Research on methanol-tolerant catalysts for the oxygen reduction reaction

M. Asteazaran[1] · G. Cespedes[2] · S. Bengió[3] · M. S. Moreno[3] · W. E. Triaca[1] ·
A. M. Castro Luna[1,2]

Abstract Direct methanol fuel cells (DMFCs) generate electricity in a clean and efficient way, so they are a valuable alternative to traditional environmentally harmful technologies. Portable power sources are one of the applications of passive DMFCs. One of the requirements in these devices is the use of high alcohol concentration. Methanol permeation across the polymer electrolyte membrane (methanol crossover) causes a loss of fuel cell efficiency as the oxygen reduction reaction (ORR) and the methanol oxidation reaction (MOR) occur simultaneously at the cathode. To develop methanol-tolerant catalysts with suitable activity, different PtM/C and PtMRu/C combinations with M = Co or Fe were prepared by a modified impregnation method. The synthesized catalysts were studied to determine the role of the components in enhancing the ORR and simultaneously discouraging the MOR. The materials were characterized by TEM, XPS and EDS. Well-distributed particles for all the catalysts were shown by TEM. XPS spectra revealed that the method produces a great amount of metallic Pt. The electrochemical characterization was carried out by linear sweep voltammetry and cyclic voltammetry, in a three-electrode electrochemical cell with a glassy carbon rotating disk electrode covered with a thin catalytic layer and a Nafion® film as the working electrode. Binary and ternary catalysts have a good activity for the ORR. However, the enhanced activity of binary catalysts is lost when the ORR is studied in the presence of methanol. Ternary catalysts containing Ru showed higher methanol-tolerance, regardless of the composition.

1 Introduction

Direct methanol fuel cells (DMFCs) are attractive devices to obtain energy in a clean and efficient manner, which is important to substitute traditional environmentally harmful technologies [1, 2]. Due to the use of methanol, an easy-handling fuel with exceptionally high energy density, DMFCs have received a large endorsement to substitute H_2/O_2 fuel cells in some application fields such as portable or signal devices [3–6]. It is widely recognized that among pure metals, platinum has the highest catalytic activity for oxygen reduction, but it is yet necessary to overcome kinetic limitations on the oxygen reduction reaction (ORR). In order to achieve catalysts with higher catalytic activity than that of Pt for the ORR, different Pt-based catalysts have been prepared and analyzed. Thus, improvements in specific activity with PtCo/C, PtNi/C or PtCr/C, and enhancement in specific activity on leached PtCo/C have been reported for ORR [7, 8]. The observed electrocatalytic effects were ascribed to several factors (interatomic spacing, preferred orientation, etc.) that contribute to enhancing the ORR. The activity enhancement has also been

✉ A. M. Castro Luna
castrolu@inifta.unlp.edu.ar; castrolu@gmail.com

1 Instituto de Investigaciones Fisicoquímicas Teóricas y Aplicadas (INIFTA), Facultad de Ciencias Exactas, UNLP-CONICET, La Plata, Argentina

2 Centro de Investigación y Desarrollo en Ciencia y Tecnología de Materiales (CITEMA), Facultad Regional La Plata, UTN, La Plata, Argentina

3 Centro Atómico Bariloche, Comisión Nacional de Energía Atómica (CAB-CNEA) and CONICET, Bariloche, Argentina

Springer

attributed to Pt segregation and to an increase of d-electron vacancies in the Pt surface layer caused by the underlying transition metal that contribute to weakening the O–O bond of adsorbed O$_2$ [8, 9].

Moreover, one of the most important challenges for the mass commercialization of DMFCs is caused by the competition between the ORR and the methanol oxidation reaction (MOR) on the Pt cathode due to methanol permeation from the anode [1, 6]. Consequently, a mixed potential is established at the electrode, which leads to a reduction in the cell voltage as well as in the cell efficiency [3]. One way of addressing the problem is to find catalysts with good performance for the ORR that are tolerant to methanol. Due to the extensive achievements in the fuel cell field, the effect of catalyst nanostructure on catalysis has attracted increasing attention [10, 11]. In previous work related to the search of a methanol-tolerant cathode catalyst for DMFCs, the authors demonstrated the importance of focusing not only on the composition but also on the catalyst synthesis method, since a different complex behavior can be obtained depending on both aspects [12].

In this work, supported nanomaterials with different compositions obtained by a modified impregnation method were systematically studied, and the role of catalyst composition for the ORR in the presence of methanol is discussed.

2 Experimental

In order to develop methanol-tolerant cathodes with suitable activity at low temperature, we prepared different carbon-supported PtM/C and PtMRu/C catalysts, with M = Co or Fe. The synthesis procedure, using slight modifications of published procedures, was the impregnation method via a seed-mediated growth, employing ethylene glycol and NaBH$_4$ as reducing agent [13].

2.1 Catalyst preparation

Following [13], a calculated amount of H$_2$PtCl$_6$, MClx (M = Fe and Co) and in some instances of RuCl$_3$ was dissolved separately in ethylene glycol. The solutions were subjected to ultrasonic agitation and purged with N$_2$ for 10 min. Subsequently, a calculated amount of functionalized carbon support (Vulcan® XC-72R) was added to a given volume of ethylene glycol and ultrasonicated for 30 min under N$_2$ flow; its pH was changed to 10 by adding NH$_4$OH. Afterward, 0.2 mL of the Pt precursor and 2 mL of a freshly prepared 0.1 M NaBH$_4$ solution were added to the carbon suspension under ultrasonic agitation to form Pt seeds. Then, the remaining precursor solutions and a given amount of NaBH$_4$ solution were added to the mixture.

Finally, the catalyst suspension was subjected to ultrasonication for 2 h under N$_2$ flow. The solid obtained after filtering the suspension was thoroughly washed with abundant distilled water and dried overnight in an oven at 70 °C. The catalysts were denoted as PtM/C or PtMRu/C. It is noteworthy to mention that the functionalization of the support was achieved after an oxidative treatment in 70 % HNO$_3$ solution at 140 °C for 2 h following [14].

2.2 Physicochemical catalysts characterization

The distribution and size particles of the supported catalysts were analyzed by high resolution transmission electron microscopy (HRTEM), their bulk compositions by energy-dispersive X-ray spectroscopy (EDS), and the surface composition and the chemical state of the active components by X-ray photoelectron spectroscopy (XPS). The electrochemical characterization was obtained employing a standard three-electrode electrochemical cell. A rotating disk electrode (RDE) of glassy carbon (0.071 cm^2 geometric area) covered with a thin layer of catalyst powder, attached by a 0.1 μm Nafion® thin film, was used as working electrode [15]. The catalyst loading on the RDE was adjusted to 28 μg$_{Pt}$cm^{-2}. A Pt foil of 1 cm^2 geometric area was used as counter electrode and a saturated calomel electrode (SCE) as reference electrode. In this work, all potentials are referred to that of the reversible hydrogen electrode (RHE). Current densities were normalized by the electrochemical surface area (ESA) obtained from the CO stripping assuming 0.42 mCcm^{-2} for one monolayer oxidation of adsorbed carbon monoxide. The CO stripping was carried out by first bubbling the solution with CO for 20 min and then with N$_2$ for another 20 min, while the potential was held at 0.05 V. Two cycles at 0.010 Vs^{-1} between 0.05 V and 0.8 or 1.1 V, depending on the catalyst composition, were performed immediately after the CO purging.

The working solution was an O$_2$-saturated 0.5 M H$_2$SO$_4$ solution with different CH$_3$OH concentrations. The electrochemical experiments were conducted at room temperature. In order to get a stable voltammetric profile, prior to ORR experiments, the potential of the working electrode was cycled at a rate of 0.1 Vs^{-1} in a N$_2$-purged 0.5 M H$_2$SO$_4$ solution for 60 cycles between 0.05 and 1.1 or 0.8 V, depending on the catalyst composition. The polarization curves were obtained starting from the open circuit potential value up to 0.050 V at a scan rate of 0.005 Vs^{-1} and a disk rotation rate of ω = 2000 rpm. The background current was measured by running the polarization curves under identical conditions to those of linear sweep voltammetry (LSV) for ORR, under N$_2$-purged 0.5 M H$_2$SO$_4$ solution. This background current was subtracted from the experimental ORR current to eliminate any

contributions of capacitive current. The current densities of the polarization curves shown in this work were calculated taking into account the geometric area of the electrode.

3 Results and discussion

3.1 Physicochemical characterization

3.1.1 EDS analysis

The atomic percentage ratios of the components in the prepared binary and ternary catalysts, determined from EDS, are shown in Table 1. The atomic percentages of Ru and Pt are almost the same, whereas the atomic percentages of Co and Fe are approximately half that of Pt.

3.1.2 XPS analysis

The Pt $4f$ and Ru $3d$ X-ray photoelectron spectra of the carbon-supported PtCoRu and PtFeRu are shown in Fig. 1a–d.

The elemental Pt $4f$ core-level spectrum is composed of two peaks that correspond to the spin–orbit split $4f_{7/2}$ and $4f_{5/2}$. For all synthesized catalysts the Pt $4f$ spectra could be deconvoluted into two pairs of doublets. The Pt $4f_{7/2}$ peaks at binding energy (BE) 71.9 eV for both trimetallic catalysts, PtFeRu/C (Fig. 1a) and PtCoRu/C (Fig. 1b), could be assigned to Pt(0). It is worth noting that the peaks are shifted apart 1 eV to more bounded states with respect to the nominal value of bulk Pt. This shift is probably due to a contribution from metal-support interaction or effects due to the small size of the nanoparticles (NP) [16]. The second Pt $4f_{7/2}$ peak for PtFeRu/C at BE = 73.9 and 73.7 eV for PtCoRu/C could be attributed to the formation of an intermediate oxide between Pt(II) and Pt(III), as has been already reported in the literature [12, 17].

In regard to Ru, the XPS spectrum is obtained in the region of Ru $3d$ core-level peak, which partially overlaps with the C $1s$ core-level peak. Despite the overlapping, the Ru $3d$ photoelectron peaks were deconvoluted into two double peaks. The Ru $3d_{5/2}$ peaks at BE = 280.1 and
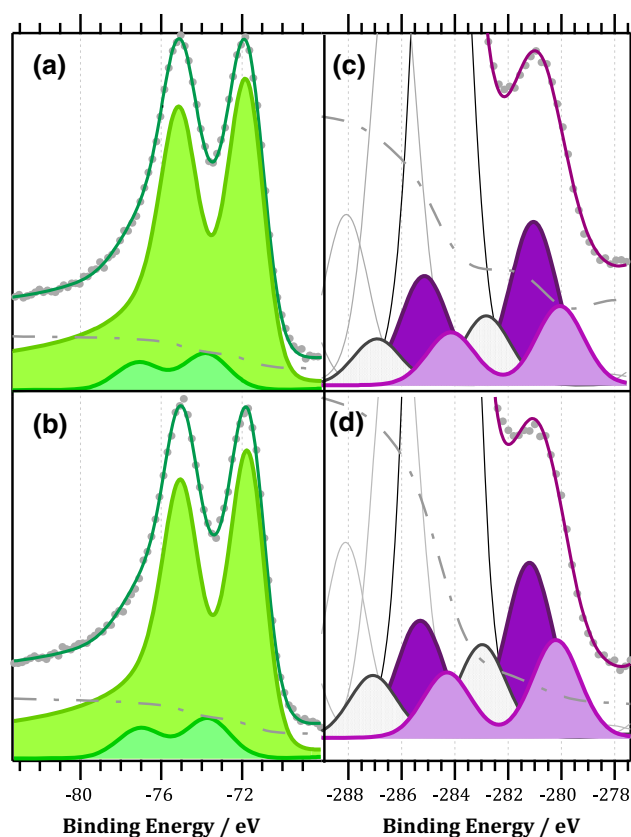

Fig. 1 XPS spectra of Pt $4f$ from PtFeRu/C (**a**) and PtCoRu/C (**b**) and of Ru $3d$ from PtFeRu/C (**c**) and PtCoRu/C (**d**)

280.2 eV for PtFeRu/C (Fig. 1c) and PtCoRu/C (Fig. 1d), respectively, are assigned to Ru (0) and the peak at BE = 281.1 and at 281.3 eV to Ru(IV), probably as RuO$_2$. The shift from the value 280.8 eV for bulk Ru(IV) could also be attributed to final state effects because of the small size of NP [12]. Additionally, a satellite peak at ca. 3 eV higher BE than the value for the Ru(IV) main peak can be identified. In Fig. 1c, d, several C $1s$ components are plotted.

The XPS peak deconvolution of C $1s$ shows four single peaks, at ca. 284.6, 286.3, 288.2 and 291 eV, which could be assigned according to increasing binding energy values: to C=C and C–C for the signal at 284.6 eV; C–O and C=O for the signal at 286.3 eV; –COO for the peak at 288.2 eV; and ester group for the peak at 291 eV.

The Co $2p$ and Fe $2p$ XPS spectra of these catalysts (not shown) exhibit a complex pattern for both Co $2p$ and Fe $2p$, each of them could barely be deconvoluted into three peaks in the region of Co $2p_{3/2}$ at around 778–781 eV composed of photoelectrons from Co(0), Co(II) and Co(III). In reference to Fe $2p$ spectra, it was also possible to identify up to three peaks in the region of Fe $2p_{3/2}$ at around 711 and 724 eV with signals composed of photoelectrons from Fe(0), Fe(II) and Fe(III).

Table 1 EDS and XPS atomic percentage ratios (%) of the synthesized catalysts

Catalyst	EDS				XPS			
	Pt	Co	Fe	Ru	Pt	Co	Fe	Ru
PtFeRu/C	41		24	35	50		12	38
PtCoRu/C	40	25		35	41	21		38
PtCo/C	75	25						
PtFe/C	77		23					

The atomic percentage ratios of the catalyst components determined by XPS, along with the values obtained by EDS, are listed in Table 1. The amount of the different components changed at the surface, as compared to those of the bulk, suggesting segregation issues [18, 19].

Summing up, we can confirm that in all synthesized catalysts Pt is mostly as Pt(0), whereas Co and Fe are largely as Co or Fe(II and III) oxides and Ru mainly as RuO_2. The relative intensities of the different components of Pt $4f_{7/2}$, Co $2p_{3/2}$, Fe $2p_{3/2}$ and Ru $3d_{5/2}$ peaks on the ternary catalysts are given in Table 2.

Table 2 Relative intensities (%) for different species as observed of XPS spectra for different catalysts

Catalyst	Pt species (Pt $4f_{7/2}$)	Relative intensities %	Co species (Co $2p_{3/2}$)	Relative intensities %	Fe species (Fe $2p_{3/2}$)	Relative intensities %	Ru species (Ru $3d_{5/2}$)	Relative intensities %
PtCoRu/C	Pt°	90	Co°	6			Ru°	27
	PtO_x	10	CoO_x	94			RuO_x	73
PtFeRu/C	Pt°	91			Fe°	8	Ru°	20
	PtO_x	9			FeO_x	92	RuO_x	80

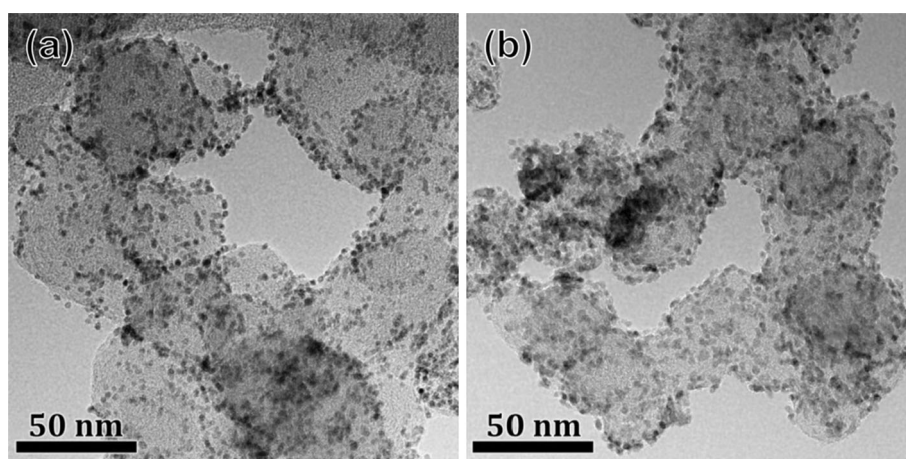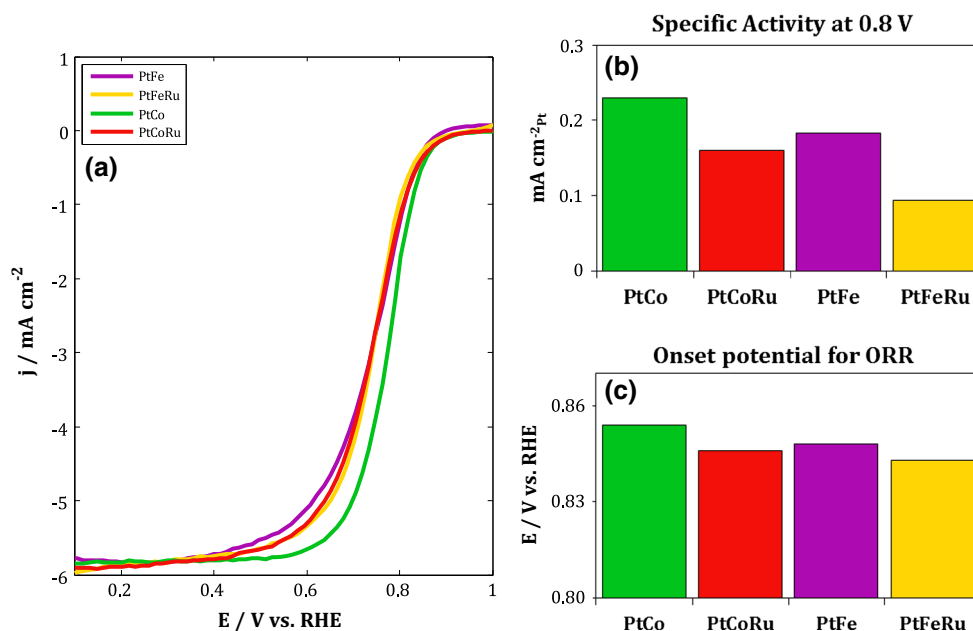**Fig. 2** TEM images of PtCo/C (**a**) and PtFeRu/C (**b**)

Fig. 3 Polarization curves for ORR on the synthesized catalysts in O_2-saturated 0.5 M H_2SO_4 at $v = 0.005$ Vs^{-1} and $\omega = 2000$ rpm (**a**); specific activity at 0.80 V (**b**); onset potential for the ORR employing the different catalysts (**c**)

3.1.3 TEM images

For all catalysts, HRTEM showed NP homogenously spread on the carbon support with narrow size distribution and uniform shape. We estimate that binary catalysts have an average particle size of ca. 3.0 nm, Fig. 2a, whereas the ternary catalysts have slightly bigger particles with an average particle size of ca. 3.5 nm, Fig. 2b.

3.2 Electrochemical performance

Typical polarization curves for ORR on PtCo/C, PtCoRu/C, PtFe/C and PtFeRu/C electrodes in an O_2-saturated 0.5 M H_2SO_4 solution, at a rotating disk rate $\omega = 2000$ rpm, are shown in Fig. 3a, the specific activity (mAcm^{-2}) at 0.80 V expressed as the kinetic current normalized by the ESA of the electrode is shown in Fig. 3b, and the onset potential for ORR in Fig. 3c. The onset potential value for the ORR on PtCo/C is close to that on Pt/C E-TEK (i.e. 0.857 V), also measured in our laboratory. Polarization curves on PtCo/C, PtCoRu/C, PtFe/C and PtFeRu/C electrodes for ORR at $\omega = 2000$ rpm in an O_2-saturated 0.5 M H_2SO_4 solution with and without 0.1 M CH_3OH, a typical concentration used in methanol tolerance studies, are shown in Fig. 4a–d, respectively. It can be noticed from the onset potential that both binary catalysts show the best catalytic activity for ORR, which can be associated with high Pt(0) content on the catalyst surface composition as reported by XPS, favoring the adsorption-reduction process of O_2. Nonetheless, both binary catalysts are less tolerant to methanol as shown in Fig. 4a, c, PtFe/C being more methanol-tolerant as claimed in [20].

On the other hand, ternary Pt-based catalysts, Fig. 4b, d, show higher methanol tolerance than binary Pt-based catalysts. It is well known that the addition of Ru enhances the MOR. The addition of Ru enhances the methanol oxidation

Fig. 4 Polarization curves for ORR in O_2-saturated 0.5 M H_2SO_4 without (*solid line*) and with (*dashed line*) 0.1 M CH_3OH at $v = 0.005$ Vs^{-1} and $\omega = 2000$ rpm on PtCo/C (*green solid line*) (**a**), PtCoRu/C (*red solid line*) (**b**), PtFe/C (*brown solid line*) (**c**) and PtFeRu/C (*yellow solid line*) (**d**). (Color figure online)
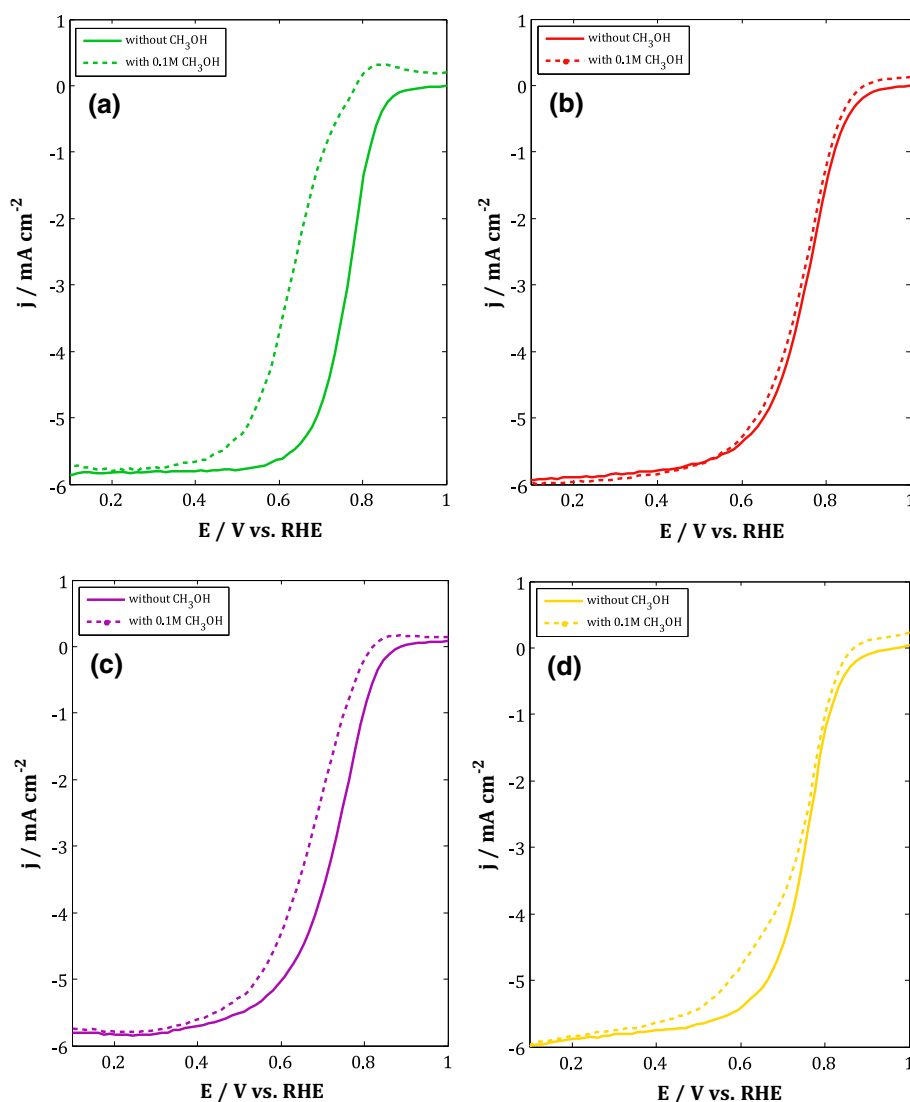
rate since methanol oxidation follows the bifunctional mechanism where Pt provides sites for C–H bond cleavage and CO adsorption, and Ru activates water to produce reactive oxides that enable the conversion of adsorbed methanol fragments to CO_2. From XPS studies on PtRu samples, it was concluded that the Ru species responsible for improving the MOR is a hydrated Ru oxide, namely, RuO_xH_y [21–23]. On the other hand, it has been recognized that a composite Pt-based catalyst capable of oxidizing methanol requires a minimum of three active Pt sites in close proximity. Accordingly, we postulate that the tolerance of our ternary catalysts is caused by (i) the presence of atoms different to Pt, blocking methanol adsorption on Pt sites causing a dilution effect [24] and (ii) the fact that according to our XPS results, in our ternary catalysts Ru is mostly as anhydrous RuO_2 with a minor content of Ru(0) and both species are not suitable for enhancing the MOR [22].

The most alcohol tolerant of the synthesized catalysts is PtCoRu/C, Fig. 4b. The presence of both Ru and Co atoms on the catalyst makes methanol adsorption unlikely given that there are not a sufficient number of active Pt sites nearby on the PtCoRu/C or the reported Ru oxide is not the hydrated oxide (RuO_xH_y) capable of improving the MOR. It is important to notice that regardless of the dilution effect, the catalytic activity of the Pt composite electrode for the ORR is not seriously hindered, since fewer nearby Pt sites are required for oxygen adsorption. The ligand effect, which concerns the electron transfer from Fe or Co to the noble metals, may explain the changes in the d band centers that weaken the O_2 adsorption strength and also help in the removal of the adsorbed O intermediates, improving the ORR [25].

In Fig. 4b, d, the polarization curves for ORR employing PtCoRu/C, and PtFeRu/C with and without methanol show that despite the similarity of both ORR polarization curves, PtCoRu/C is the most methanol-tolerant cathode. Notably, taking into account the similar Ru content on both ternary catalysts, shown in Table 1, the higher methanol tolerance of PtMRu/C catalysts could be attributed to appreciable Ru content.

4 Conclusions

In this study, PtCoRu/C and PtFeRu/C ternary electrocatalysts together with the binary PtCo/C and PtFe/C combinations were prepared by a modified impregnation method via a seed-mediated growth, with ethylene glycol as solvent and sodium borohydride as reducing agent. The catalytic NPs were well dispersed on the carbon support. The trimetallic catalysts exhibit similar ORR activity to that of Pt and a superior methanol tolerance than Pt or

binary Pt combinations. Among binary catalysts, PtFe/C is more methanol-tolerant.

Trimetallic PtMRu/C catalysts show the lowest activity towards methanol oxidation. The high methanol tolerance of the PtMRu/C catalysts during the ORR can be explained by the low activity for methanol oxidation, originated from the composition effect that causes changes in the distribution of active sites, and to the presence of RuO_2, which is inactive for MOR enhancement.

References

1. Corti HR, Gonzalez ER (2014) Direct alcohol fuel cells materials, performance, durability and applications. Springer, Amsterdam. doi:10.1007/978-94-007-7708-8
2. Aricò AS, Baglio V, Antonucci V (2009) Direct methanol fuel cells: history, status and perspectives. In: Liu H, Zhang J (eds) Electrocatalysis of direct methanol fuel cells: from fundamentals to applications. Wiley, Weinheim, pp 1–78. doi:10.1002/9783527627707.ch1
3. Faghri A, Guo Z (2008) An innovative passive DMFC technology. Appl Therm Eng 28:1614–1622. doi:10.1016/j.applthermaleng.2007.10.024
4. Baglio V, Antonucci V, Aricò AS (2010) Status of technology and perspectives for portable applications of direct methanol fuel cells. In: Pignataro B (ed) Ideas in Chemistry and Molecular Sciences: Advances in Nanotechnology, Materials and Devices. Wiley-VCH Verlag GmbH & Co. KGaA, Weinheim. doi:10.1002/9783527630530.ch11
5. Zhao TS, Chen R, Yang WW, Xu C (2009) Small direct methanol fuel cells with passive supply of reactants. J Power Sources 191:185–202. doi:10.1016/j.jpowsour.2009.02.033
6. Baglio V, Stassi A, Matera FV, Antonucci V, Aricò AS (2009) Investigation of passive DMFC mini-stacks at ambient temperature. Electrochim Acta 54:2004–2009. doi:10.1016/j.electacta.2008.07.061
7. Murthi VS, Urian RC, Mukerjee S (2004) Oxygen reduction kinetics in low and medium temperature acid environment: correlation of water activation and surface properties in supported Pt and Pt alloy electrocatalysts. J Phys Chem B 108:11011–11023. doi:10.1021/jp048985k
8. Gasteiger HA, Kocha SS, Sompalli S, Wagner FT (2005) Activity benchmarks and requirements for Pt, Pt-alloys, and non-Pt oxygen reduction catalysts for PEMFCs. Appl Catal B 56:9–35. doi:10.1016/j.apcatb.2004.06.021
9. van der Vlie DF, Wang C, Li D, Paulikas AP, Greeley J, Rankin RB, Strmcnik D, Tripkovic D, Markovic NM, Stamenkovic VR (2012) Unique electrochemical adsorption properties of Pt-skin surfaces. Angew Chem Int Ed 51:3139–3142. doi:10.1002/anie.201107668
10. Yang J, Zhou W, Cheng CH, Lee JL, Liu Z (2010) Pt-decorated PdFe nanoparticles as methanol-tolerant oxygen reduction electrocatalyst. ACS Appl Mater Interfaces 2:119–126. doi:10.1021/am900623e

11. Antolini E, Lopes T, Gonzalez ER (2008) An overview of platinum-based catalysts as methanol-resistant oxygen reduction materials for direct methanol fuel cells. J Alloys Compd 461:253–262. doi:10.1016/j.jallcom.2007.06.077

12. Asteazaran M, Bengió S, Triaca WE, Castro Luna AM (2014) Methanol tolerant electrocatalysts for the oxygen reduction reaction. J Appl Electrochem 44:1271–1278. doi:10.1007/s10800-014-0748-1

13. Spanos I, Kirkensgaard JJK, Mortensen K, Arenz M (2014) Investigating the activity enhancement on Pt_xCo_{1-x} alloys induced by a combined strain and ligand effect. J Power Sources 245:908–914. doi:10.1016/j.jpowsour.2013.07.023

14. Bonesi AR, Moreno MS, Triaca WE, Castro Luna AM (2010) Modified catalytic materials for ethanol oxidation. Int J Hydrogen Energy 35:5999–6004. doi:10.1016/j.ijhydene.2009.12.093

15. Paulus UA, Schmidt TJ, Gasteiger HA, Behm RJ (2001) Oxygen reduction on a high-surface area Pt/Vulcan carbon catalyst: a thin-film rotating ring-disk electrode study. J Electroanal Chem 495:134–145. doi:10.1016/S0022-0728(00)00407-1

16. Aricò AS, Shukla A, Kim H, Park S, Min M, Antonucci V (2001) An XPS study on oxidation states of Pt and its alloys with Co and Cr and its relevance to electroreduction of oxygen. Appl Surf Sci 172:33–40. doi:10.1016/S0169-4332(00)00831-X

17. Jung MC, Kim HD, Han M, Jo W, Kim DC (1999) X-ray photoelectron spectroscopy study of Pt-oxide thin films deposited by reactive sputtering using O_2/Ar gas mixtures. Jpn J Appl Phys 38:4872–4875. doi:10.1143/JJAP.38.4872

18. Stamenkovic VR, Mun BS, Arenz M, Mayrhofer KJJ, Lucas CS, Wang G, Ross PN, Markovic NM (2007) Trends in electrocatalysis on extended and nanoscale Pt-bimetallic alloy surfaces. Nat Mater 6:241–247. doi:10.1038/nmat1840

19. Wang C, Wang G, van der Vliet D, Chang KC, Markovic NM, Stamenkovic VR (2010) Monodisperse Pt_3Co nanoparticles as electrocatalyst: the effects of particle size and pretreatment on electrocatalytic reduction of oxygen. Phys Chem Chem Phys 12:6933–6939. doi:10.1039/c000822b

20. Castro Luna AM, Bonesi A, Triaca WE, Baglio V, Antonucci V, Aricò AS (2008) Pt–Fe cathode catalysts to improve the oxygen reduction reaction and methanol tolerance in direct methanol fuel cells. J Solid State Electrochem 12:643–649. doi:10.1007/s10008-007-0334-0

21. Raman RK, Shukla AK, Gayen A, Hegde MS, Priolkar KR, Sarode PR, Emura S (2006) Tailoring a Pt–Ru catalyst for enhanced methanol electro-oxidation. J Power Sources 157:45–55. doi:10.1016/j.jpowsour.2005.06.031

22. Long JW, Stroud RM, Swider-Lyons KE, Rolison DR (2000) How to make electrocatalysts more active for direct methanol oxidation-avoid PtRu bimetallic alloys! J Phys Chem B 104:9772–9776. doi:10.1021/jp001954e

23. Raman RK, Shukla AK, Gayen A, Hegde MS, Priolkar KR, Sarode PR, Emura S (2006) Tailoring a Pt–Ru catalyst for enhanced methanol electro-oxidation. J Power Sources 157:45–55. doi:10.1016/j.jpowsour.2005.06.031

24. Salgado JRC, Antolini E, Gonzalez ER (2005) Carbon supported Pt–Co alloys as methanol-resistant oxygen-reduction electrocatalysts for direct methanol fuel cells. Appl Catal B 57:283–290. doi:10.1016/j.apcatb.2004.11.009

25. Cho YH, Kimb OH, Chung DY, Choe H, Choc YH, Sung YE (2014) PtPdCo ternary electrocatalyst for methanol tolerant oxygen reduction reaction in direct methanol fuel cell. Appl Catal B 154–155:309–315. doi:10.1016/j.apcatb.2014.02.016